Full-Wave Analysis of a Nonradiative Dielectric Waveguide with a Pseudochiral Ω-Slab

António L. Topa, Carlos R. Paiva, *Member, IEEE,* and Afonso M. Barbosa, *Senior Member, IEEE*

***Abstract*—This paper presents a new microwave device—a nonradiative dielectric (NRD) waveguide with a dielectric pseudochiral Ω-slab—the Ω-NRD waveguide. A rigorous full-wave analysis is presented and the modal equations for the longitudinal-section magnetic (LSM) and longitudinal-section electric (LSE) modes are derived. The dispersion curves and operational diagrams for the first hybrid LSM modes are presented. The effect of the pseudochiral Ω-medium is discussed. New interesting modal features are revealed, showing that the propagation characteristics may differ considerably from the common isotropic case.**

***Index Terms*— Modal analysis, nonradiative dielectric waveguide, Ω-media, pseudochiral.**

I. Introduction

PSEUDOCHIRAL Ω-media have recently generated (due to their new electromagnetic characteristics) considerable attention in the literature [1]-[6]. The applications of the pseudochiral or Ω-medium in the microwave and millimeter-wave regimes have prompted a renewed interest over the last years. This new type of complex medium, which is nonchiral, can be obtained by doping a host isotropic medium with Ω-shaped conducting microstructures where both the loop and stamps lie in the same plane. As a result, the electric field induces not only electric, but also magnetic polarizations.

The field displacement phenomena occurring in pseudochiral Ω-media has been reported in [6] and electromagnetic-wave interaction with pseudochiral materials has suggested several new applications such as a reciprocal phase shifter [2].

On the other hand, the nonradiative dielectric (NRD) waveguide technology is very promising for microwave and millimeter-wave integrated circuits [7]–[12]. As is well known, the NRD waveguide (using an isotropic dielectric) was proposed to overcome the radiation losses at curved sections and discontinuities of most dielectric waveguides. It resembles the usually termed H-guide [13], but with the parallel metal plates separated by a distance smaller than a half-wavelength. In this way, the electromagnetic field cannot propagate between them due to the cutoff condition. Therefore, the suppression of undesirable radiation is achieved with the advantage of a strong reduction in interference and radiation problems in integrated circuits.

Manuscript received June 17, 1997; revised March 9, 1998. This work was supported in part by the Praxis XXI Program under Project 2/2.1/TIT/1663/95.

The authors are with the Department of Electrical and Computer Engineering, Instituto Superior Técnico (IST), Technical University of Lisbon, Lisbon 1096, Portugal, and also with the Institute for Telecommunications, Lisbon 1096, Portugal.

Publisher Item Identifier S 0018-9480(98)06145-6.

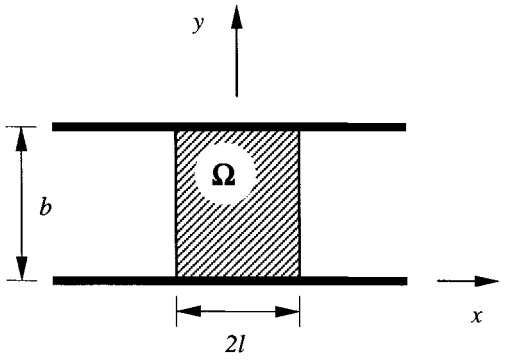

Fig. 1. Geometry of an NRD waveguide with a pseudochiral Ω-slab—the Ω-NRD-guide. The surrounding medium is the air.

The devices which have been proposed so far with the NRD technology use isotropic, ferrite [11], [14] or anisotropic materials [15].

This paper, which is an extension of [16], addresses for the first time the problem of electromagnetic-wave propagation in an NRD waveguide where the isotropic slab is replaced by a pseudochiral Ω-medium slab—the Ω-NRD waveguide. It is shown that this type of waveguide supports longitudinal-section electric (LSE) and longitudinal-section magnetic (LSM) hybrid modes. In this paper, the modal equations for the LSE and LSM modes are derived, and the dispersion curves and the corresponding operational diagrams are presented. The effect of including Ω-shaped microstructures is analyzed, and new interesting modal features are revealed, showing that the propagation characteristics may considerably differ from the common isotropic case.

II. Field Equations

The structure proposed for consideration consists of a pseudochiral rectangular Ω-strip located between two parallel metal plates, as depicted in Fig. 1. The electromagnetic properties of the pseudochiral Ω-medium are better represented by the following constitutive relations [1]:

$$\boldsymbol{D} = \bar{\varepsilon} \cdot \boldsymbol{E} + \overline{\Omega}_{em} \cdot \boldsymbol{B} \tag{1a}$$

$$\boldsymbol{H} = \bar{\mu}^{-1} \cdot \boldsymbol{B} + \overline{\Omega}_{me} \cdot \boldsymbol{E}. \tag{1b}$$

However, by introducing a normalized magnetic field $\mathcal{H}$ along with normalized electric displacement $\mathcal{D}$ and normalized magnetic flux density $\mathcal{B}$—all with electric-field dimensions—such that

$$\mathcal{H} = Z_0 \boldsymbol{H} \tag{2a}$$

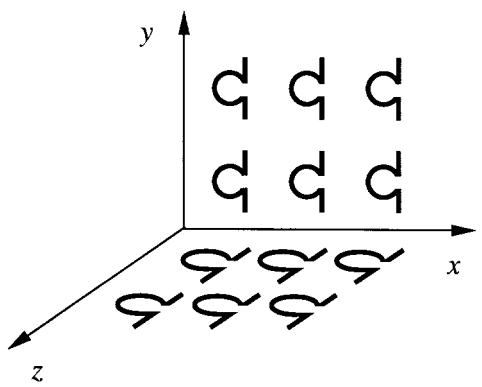

Fig. 2. Uniaxial pseudochiral Ω-medium—spatial orientation of the two ensembles of Ω-shaped conducting microstructures in the hosting isotropic material.

$$\mathcal{D} = \frac{1}{\varepsilon_0}\,\boldsymbol{D} \tag{2b}$$

$$\mathcal{B} = \frac{Z_0}{\mu_0}\,\boldsymbol{B} \tag{2c}$$

with $Z_0 = \sqrt{\mu_0/\varepsilon_0}$, the constitutive relations (1) can be rewritten as in [19] and [20], i.e.,

$$\mathcal{D} = \overline{\varepsilon}' \cdot \boldsymbol{E} + \overline{\xi} \cdot \mathcal{H} \tag{3a}$$

$$\mathcal{B} = \overline{\zeta} \cdot \boldsymbol{E} + \overline{\mu}' \cdot \mathcal{H} \tag{3b}$$

where $\overline{\varepsilon}'$, $\overline{\mu}'$, $\overline{\xi}$, and $\overline{\zeta}$ are dimensionless constitutive tensors, which obey the following relations:

$$\overline{\varepsilon}' = \frac{1}{\varepsilon_0}\,(\overline{\varepsilon} - \overline{\Omega}_{em} \cdot \overline{\mu} \cdot \overline{\Omega}_{me}) \tag{4a}$$

$$\overline{\xi} = \frac{Y_0}{\varepsilon_0}\,\overline{\Omega}_{em} \cdot \overline{\mu} \tag{4b}$$

$$\overline{\zeta} = -\frac{Z_0}{\mu_0}\,\overline{\mu} \cdot \overline{\Omega}_{me} \tag{4c}$$

$$\overline{\mu}' = \frac{1}{\mu_0}\,\overline{\mu}. \tag{4d}$$

Using normalized distances marked with primes (e.g., $x' = k_0 x$, $y' = k_0 y$, $z' = k_0 z$ with $k_0 = \omega\sqrt{\varepsilon_0\mu_0}$) and assuming time-harmonic field variation of the form $\exp(j\omega t)$, then from Maxwell's curl equations for source-free regions together with (3), one may write

$$-j\nabla' \times \mathcal{H} = \overline{\varepsilon}' \cdot \boldsymbol{E} \cdot \overline{\xi} \cdot \mathcal{H} \tag{5a}$$

$$j\nabla' \times \boldsymbol{E} = \overline{\zeta} \cdot \boldsymbol{E} + \overline{\mu}' \cdot \mathcal{H} \tag{5b}$$

where $\nabla' = \nabla/k_0$.

Hereafter, we only consider the particular case of a pseudochiral medium where two sets of Ω-shaped microstructures with different orientations are included in the host isotropic medium. The relative orientation of these two ensembles is depicted in Fig. 2.

For this geometry, the relative electric permittivity and relative magnetic permeability tensors have the following uniaxial form:

$$\overline{\varepsilon}' = \varepsilon_{\|}\hat{\boldsymbol{x}}\hat{\boldsymbol{x}} + \varepsilon_{\perp}(\hat{\boldsymbol{y}}\hat{\boldsymbol{y}} + \hat{\boldsymbol{z}}\hat{\boldsymbol{z}}) \tag{6a}$$

$$\overline{\mu}' = \mu_{\|}\hat{\boldsymbol{x}}\hat{\boldsymbol{x}} + \mu_{\perp}(\hat{\boldsymbol{y}}\hat{\boldsymbol{y}} + \hat{\boldsymbol{z}}\hat{\boldsymbol{z}}). \tag{6b}$$

Moreover, the dimensionless magnetoelectric tensors $\overline{\xi}$ and $\overline{\zeta}$ have the following dyadic representation [18]:

$$\overline{\xi} = j\Omega(\hat{\boldsymbol{y}}\hat{\boldsymbol{z}} - \hat{\boldsymbol{z}}\hat{\boldsymbol{y}}) \tag{7a}$$

$$\overline{\zeta} = j\Omega(\hat{\boldsymbol{y}}\hat{\boldsymbol{z}} - \hat{\boldsymbol{z}}\hat{\boldsymbol{y}}) \tag{7b}$$

where Ω is a pseudochiral dimensionless coefficient which is related with the pseudochiral admittance Ω_c [1] according to the following expression:

$$\Omega = \mu_{\perp}\,\frac{\Omega_c}{Y_0}. \tag{8}$$

In accordance with Fig. 2, one always has $\Omega > 0$. For $\Omega < 0$, the Ω structures of Fig. 2 should be drawn turned around.

Therefore, the pseudochiral medium has no preferred direction in the y–z plane. Such a medium can be termed *uniaxial Ω-medium* [17], [18] since there exists only one particular direction—normal to the interfaces—i.e., the x-direction. Moreover, since one has $\overline{\zeta} = -\overline{\xi}^{\mathrm{T}}$, the pseudochiral uniaxial Ω-medium is reciprocal, as was expected.

Considering forward plane-wave propagation of the form $\exp(-j\beta z')$, where $\beta = k_z/k_0$ is the normalized longitudinal wavenumber, one has

$$\nabla' = \partial_{x'}\hat{\boldsymbol{x}} + \partial_{y'}\hat{\boldsymbol{y}} - j\beta\hat{\boldsymbol{z}} \tag{9}$$

where $\partial_{x'}$ stands for $\partial/\partial x'$ and $\partial_{y'}$ for $\partial/\partial y'$. After substituting (6) and (7) into Maxwell's equations (5), one obtains (for the field in the pseudochiral slab) the following relations:

$$-j(\partial_{y'}\mathcal{H}_z + j\beta\mathcal{H}_y) = \varepsilon_{\|}E_x \tag{10a}$$

$$j(\partial_{x'}\mathcal{H}_z + j\beta\mathcal{H}_x) = \varepsilon_{\perp}E_y + j\Omega\mathcal{H}_z \tag{10b}$$

$$-j(\partial_{x'}\mathcal{H}_y - \partial_{y'}\mathcal{H}_x) = \varepsilon_{\perp}E_z - j\Omega\mathcal{H}_y \tag{10c}$$

and

$$j(\partial_{y'}E_z + j\beta E_y) = \mu_{\|}\mathcal{H}_x \tag{11a}$$

$$-j(\partial_{x'}E_z + j\beta E_z) = \mu_{\perp}\mathcal{H}_y + j\Omega E_z \tag{11b}$$

$$j(\partial_{x'}E_y - \partial_{y'}E_x) = \mu_{\perp}\mathcal{H}_z - j\Omega E_y \tag{11c}$$

respectively.

It can be easily shown that for this type of geometry and with these constitutive relations, the Ω-NRD waveguide only supports LSE (i.e., with $E_x = 0$) and LSM (i.e., with $\mathcal{H}_x = 0$) hybrid modes. In fact, as is well known, in the case of a uniaxial Ω-slab with the same configuration, the guided modes are pure TE and TM modes [17], [18]. Moreover, the perfectly conducting planes to be located at $y = 0$, b will not affect the x-directed field components. Hence, from (10) and (11), one can see that there is no coupling between E_x and $\mathcal{H}_x$ field components.

Therefore, for the LSM modes (former TM modes), taking $\mathcal{H}_x = 0$ in (10) and (11) and choosing $\mathcal{H}_y$ as the supporting field component, the following differential equation can be easily derived:

$$\partial_{x'}^2\mathcal{H}_y + \frac{\varepsilon_{\perp}}{\varepsilon_{\|}}\,\partial_{y'}^2\mathcal{H}_y = -\left(\varepsilon_{\perp}\mu_{\perp} - \Omega^2 - \frac{\varepsilon_{\perp}}{\varepsilon_{\|}}\,\beta^2\right)\mathcal{H}_y. \tag{12}$$

Moreover, taking $\nabla' \cdot \mathcal{B} = 0$ in (11), all the other field components can be expressed in terms of the supporting field component $\mathcal{H}_y$ according to

$$\mathcal{H}_z = -j\,\frac{1}{\beta}\,\partial_{y'}\mathcal{H}_y \tag{13a}$$

$$E_x = -\frac{1}{\beta\varepsilon_{\|}}\,(\partial^2_{y'}\mathcal{H}_y - \beta^2\mathcal{H}_y) \tag{13b}$$

$$E_y = \frac{1}{\beta\varepsilon_{\perp}}\,(\partial_{y'}\partial_{x'}\mathcal{H}_y - \Omega\partial_{y'}\mathcal{H}_y) \tag{13c}$$

$$E_z = -j\,\frac{1}{\varepsilon_{\perp}}\,(\partial_{x'}\mathcal{H}_y - \Omega\mathcal{H}_y). \tag{13d}$$

On the other hand, for the LSE modes (former TE modes), taking $E_x = 0$ in (10) and (11) and choosing E_y as the supporting field component, the following differential equation is derived instead:

$$\partial^2_{x'}E_y + \frac{\mu_{\perp}}{\mu_{\|}}\,\partial^2_{y'}E_y = -\left(\mu_{\perp}\varepsilon_{\perp} - \Omega^2 - \frac{\mu_{\perp}}{\mu_{\|}}\,\beta^2\right)E_y. \tag{14}$$

In this case, all the other field components can be expressed in terms of E_y, by taking $\nabla' \cdot \mathcal{D} = 0$ in (10)

$$E_z = -j\,\frac{1}{\beta}\,\partial_{y'}E_y \tag{15a}$$

$$\mathcal{H}_x = \frac{1}{\beta\mu_{\|}}\,(\partial^2_{y'}E_y - \beta^2 E_y) \tag{15b}$$

$$\mathcal{H}_y = -\frac{1}{\beta\mu_{\perp}}\,(\partial_{y'}\partial_{x'}E_y + \Omega\partial_{y'}E_y) \tag{15c}$$

$$\mathcal{H}_z = j\,\frac{1}{\mu_{\perp}}\,(\partial_{x'}E_y + \Omega E_y). \tag{15d}$$

III. Modal Equations

As is well known from the isotropic case, the LSM_{01} mode is the most interesting mode for applications due to its monotonous decrease in wall attenuation with frequency. However, for the new pseudochiral structure, we will also proceed to the analysis of LSE_{mn} modes.

Starting with the LSM_{mn} modes, one may express $\mathcal{H}_y$ as a product of two separate-variable functions in the form

$$\mathcal{H}_y = f(x')g(y')\exp(-j\beta z') \tag{16}$$

such that

$$\partial^2_{x'}f + \beta_x^2 f(x') = 0 \tag{17a}$$

$$\partial^2_{y'}g + \beta_y^2 g(y') = 0 \tag{17b}$$

with $\beta_x = k_x/k_0$ and $\beta_y = k_y/k_0$, and substituting back into (13), the following relations between the normalized wavenumbers can be obtained:

$$h^2 + \frac{\varepsilon_{\perp}}{\varepsilon_{\|}}\,(\beta_y^2 + \beta^2) = \varepsilon_{\perp}\mu_{\perp} - \Omega^2 \tag{18}$$

$$-\alpha^2 + \beta_y^2 + \beta^2 = 1. \tag{19}$$

One has $\beta_x = h$ for $|x'| < l'$ while for $|x'| > l'$, one should take $\beta_x = -j\alpha$ with $\alpha > 0$. According to the boundary conditions on the perfectly electric conductor planes, i.e.,

$$E_x(y' = 0, b') = 0 \tag{20a}$$

$$E_z(y' = 0, b') = 0 \tag{20b}$$

one may write

$$g(y') = G\sin(\beta_y y') \tag{21}$$

where $(n = 1, 2, 3, \cdots)$

$$\beta_y = n\,\frac{\pi}{b'} \tag{22}$$

with $b' = k_0 b$. The n index gives the number of half-waves along y. All the NRD waveguide components usually preserve the vertical symmetry, so that, in general, a $n = 1$ y-dependence may be assumed.

Equations (13c) and (13d) show that the electric-field components E_y and E_z are asymmetric with respect to the geometrical symmetry plane of the waveguide—i.e., $x' = 0$. Therefore, one should write

$$f(x') = \begin{cases} F_1\exp[\alpha(x' + l')], & x' < -l' \\ F_2[\cos(hx') + R\sin(hx')], & -l' < x' < l' \\ F_3\exp[-\alpha(x' - l')], & l' < x' \end{cases} \tag{23}$$

In order to obtain the modal equations, it is necessary to use continuity conditions at both planes $x' = \pm l'$. Enforcing the boundary conditions at $x' = \pm l'$, one obtains, according to (13b) and (13d)

$$\frac{1}{\varepsilon_{\perp}}\,[\partial_{x'}f(x' = \pm l'^{-}) - \Omega f(x' = \pm l'^{-})] = \partial_{x'}f(x' = \pm l'^{+}) \tag{24a}$$

$$f(x' = \pm l'^{-}) = f(x' = \pm l'^{+}) \tag{24b}$$

Hence, the modal equation for the LSM hybrid modes can be easily derived

$$[h\cot(hl') + \alpha\epsilon_{\perp}]\cdot[h\tan(hl') - \alpha\varepsilon_{\perp}] + \Omega^2 = 0. \tag{25}$$

For the LSE hybrid modes, a similar derivation could be done. However, for the boundary conditions at $x' = \pm l'$, instead of (24), the following relations apply:

$$\frac{1}{\mu_{\perp}}\,[\partial_{x'}f(x' = \pm l'^{-}) - \Omega f(x' = \pm l'^{-})] = \partial_{x'}f(x' = \pm l'^{+}) \tag{26a}$$

$$f(x' = \pm l'^{-}) = f(x' = \pm l'^{+}). \tag{26b}$$

leading to a dual modal equation for the LSE modes

$$[h\cot(hl') + \alpha\mu_{\perp}]\cdot[h\tan(hl') - \alpha\mu_{\perp}] + \Omega^2 = 0. \tag{27}$$

However, in this case, the normalized transverse wavenumber in the slab, i.e., h, should be given by

$$h^2 + \frac{\mu_{\perp}}{\mu_{\|}}\,(\beta_y^2 + \beta^2) = \mu_{\perp}\varepsilon_{\perp} - \Omega^2 \tag{28}$$

instead of (18).

The boundary conditions (24) and (26) once again show that there is no coupling between the LSE and LSM hybrid modes, since (24) and (26) can be satisfied by each one of these type of modes independently.

One should stress that when the pseudochiral effect vanishes, i.e., when $\Omega = 0$, (25) and (27) become a product of two

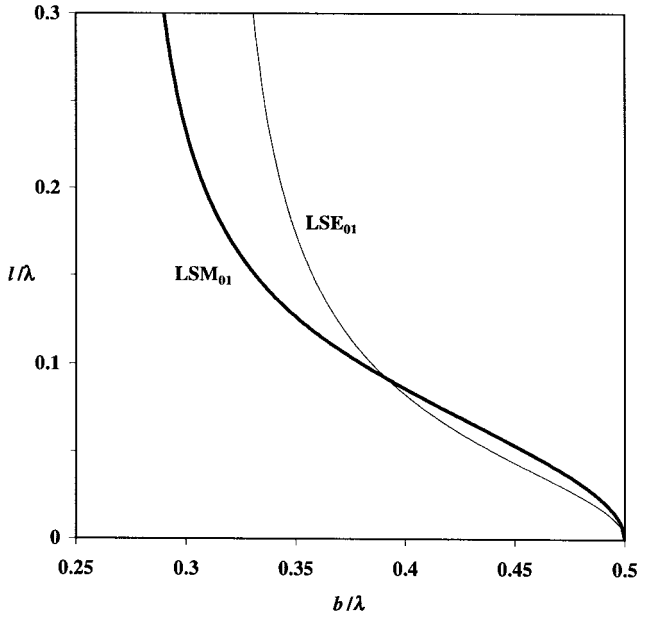

Fig. 3. Operational diagram for the LSM_{01} and LSE_{01} hybrid modes of a Ω-NRD waveguide with $\varepsilon_{||}$ =2, $\varepsilon_{\perp}=3$, $\mu_{||}=1$, $\mu_{\perp}=2$, and $\Omega=1$.

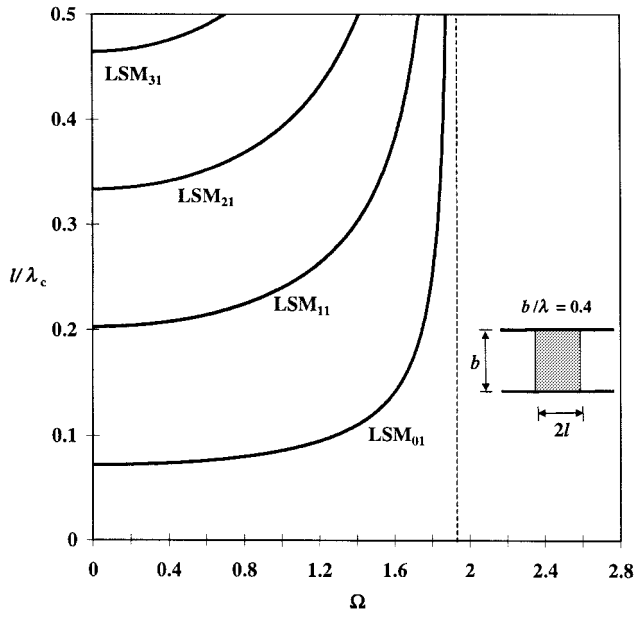

Fig. 4. Variation of the cutoff parameter l/λ_c with Ω for the first LSM modes of an Ω-NRD waveguide with $\varepsilon_{||}=2$, $\varepsilon_{\perp}=3$, $\mu_{||}=1$, $\mu_{\perp}=2$, and $b/\lambda=0.4$.

elementary modal equations. Henceforth, in that case, the even and odd LSE and LSM modes appear in the waveguide—i.e., the plane $x'=0$ becomes a symmetry plane.

Finally, the m index (with $m=0,1,2,\cdots$) appearing in the descriptors LSE_{mn} and LSM_{mn} gives the order of the eigensolution in (25) and (27).

IV. Numerical Results

The numerical results presented in this section were obtained by solving modal equations (25) and (27) together with (18) and (19). Since this waveguide is a *semi-open* structure, the cutoff can be determined either by the closed-waveguide cutoff condition (NRD-guide regime), i.e., $\beta=0$, or by the open-waveguide cutoff condition (H-guide regime), i.e., $\alpha=0$, depending on the value.

In this example and for the sake of numerical application, a pseudochiral Ω-slab with $\varepsilon_{||}=2$, $\varepsilon_{\perp}=3$, $\mu_{||}=1$, $\mu_{\perp}=2$, and with arbitrary pseudochiral parameter Ω is considered. In fact, if one inserts Ω-inclusions uniaxially (as described in Fig. 2) into an isotropic host medium, there will be an increase in the permittivity and permeability in the lateral directions [18]. It thus follows that $\varepsilon_{||}<\varepsilon_{\perp}$ and $\mu_{||}<\mu_{\perp}$.

An accurate choice of the geometrical and physical parameters of the waveguide, such as the dielectric strip height and width as well as the permittivity and permeability of the dielectric is required in order to optimize the transmission characteristics of the NRD waveguide. The operational diagrams are usually employed for that purpose [7].

Therefore, Fig. 3 shows the operational diagram for the first LSM and LSE hybrid modes when $\Omega=1$. One should note that there is a crossing point between the two curves. This shows that, in fact, there is no coupling between the two types of modes. Moreover, only for some values of the parameter b/λ, the LSM_{01} mode is the fundamental mode.

The variation of the cutoff parameter l/λ_c with the pseudochiral Ω parameter for the first LSM_{m1} modes is shown in Fig. 4 for $b/\lambda=0.4$. Hence, in this case, the cutoff of each mode is determined by the closed waveguide cutoff condition (i.e., $\beta=0$). The vertical dashed line corresponds to $h=0$, and sets a limiting value for Ω above which there is no guided wave propagation

$$\Omega_l=\sqrt{\varepsilon_{\perp}\mu_{\perp}-\frac{\varepsilon_{\perp}}{\varepsilon_{||}}\beta_y^2} \tag{29}$$

where β_y is given by (21) with $n=1$.

The variation of the cutoff parameter b/λ_c with Ω is depicted in Fig. 5 for the same modes considered in Fig. 4. In this case, the form factor is $b/\lambda=1.2$. The thin line corresponds to an under-limiting value for b/λ_c, which is reached whenever $h\to 0$. This value is given by

$$b/\lambda_l=\frac{1}{2\sqrt{\dfrac{\varepsilon_{||}}{\varepsilon_{\perp}}\left(\varepsilon_{\perp}\mu_{\perp}-\Omega^2\right)}} \tag{30}$$

and was obtained by making $h=0$ in (17) when $\beta=0$. Above $b/\lambda=0.5$, the cutoff is determined by the open waveguide mechanism (i.e., $\alpha=0$), and the vertical thin line corresponds to the following maximum value for Ω:

$$\Omega_{\max}=\sqrt{\varepsilon_{\perp}\mu_{\perp}-\frac{\varepsilon_{\perp}}{\varepsilon_{||}}}. \tag{31}$$

This value was now obtained by making $h=0$ in (17) and taking $\alpha=0$.

The operational diagram for the Ω-NRD waveguide is depicted in Fig. 6 for several values of the pseudochiral Ω parameter. Above the radiation-suppression condition (i.e., for $b/\lambda<0.5$), all the curves are independent from b/λ. The

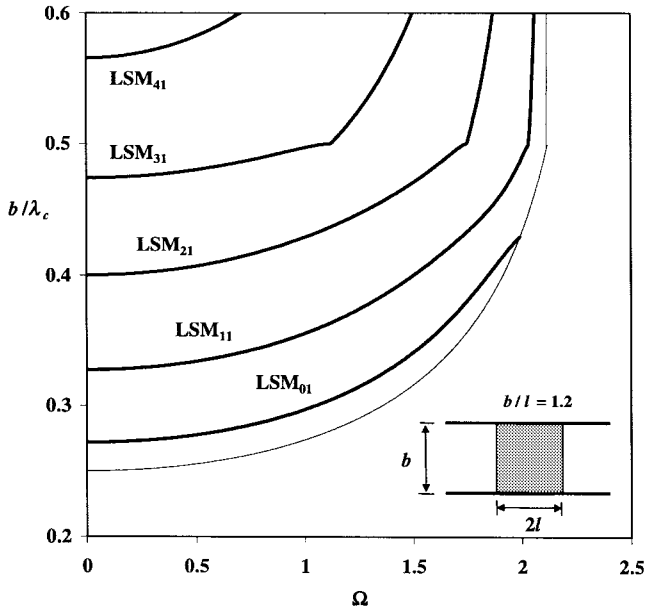

Fig. 5. Variation of the cutoff parameter b/λ_c with Ω for the first propagating LSM modes of an Ω-NRD waveguide with $\varepsilon_{\|} = 2$, $\varepsilon_{\perp} = 3$, $\mu_{\|} = 1, \mu_{\perp} = 2$, and $b/\lambda = 1.2$.

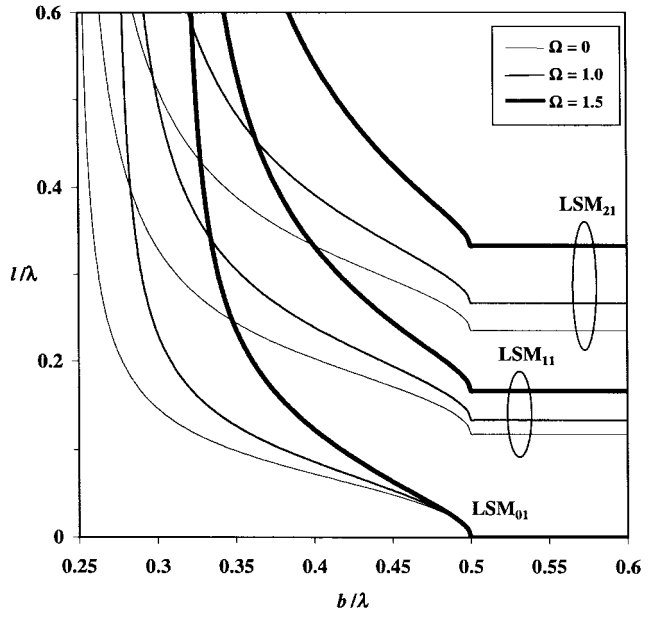

Fig. 6. Operational diagram for the first propagating LSM modes of an Ω-NRD waveguide with $\varepsilon_{\|} = 2$, $\varepsilon_{\perp} = 3$, $\mu_{\|} = 1$, and $\mu_{\perp} = 2$ for several values of Ω. The thinner line corresponds to the nonpseudochiral case.

thinner line represents the nonpseudochiral case, i.e., $\Omega = 0$, when the medium simply becomes uniaxial anisotropic.

If the LSE modes are not taken into account, the bandwidth for single-mode operation in the Ω-NRD waveguide is limited below by the LSM_{01}-mode cutoff, and above by either the LSM_{11}-mode cutoff or the radiation-suppression condition ($b/\lambda < 0.5$). As one can see, even with the inclusion of Ω-shaped microstructures, the fundamental LSM_{01} mode is the only mode that has no cutoff frequency for $b/\lambda > 0.5$. All the other modes suffer an increase of their cutoff frequency due to the pseudochirality. Therefore, under certain circumstances,

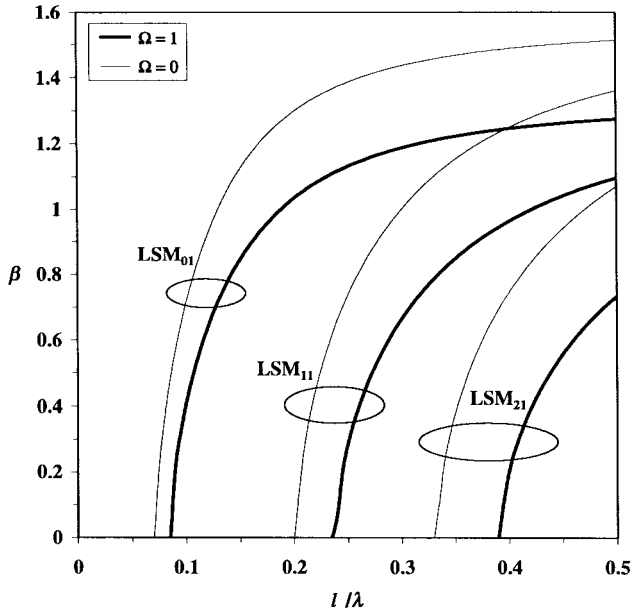

Fig. 7. Variation of the longitudinal wavenumber β with l/λ for the first propagating LSM modes of the Ω-NRD waveguide of Fig. 4. The thick lines correspond to $\Omega = 1.0$, while the thin lines correspond to the nonpseudochiral case.

the bandwidth for single-mode operation (defined in accordance with [7]) may be increased by the use of a pseudochiral Ω-slab.

In Fig. 7, the variation of the longitudinal wavenumber β with l/λ is depicted for $\beta/\lambda = 0.4$ and $\Omega = 0, 1$. The thin lines again correspond to the nonpseudochiral case. In the high-frequency regime (i.e., when $l/\lambda \to \infty$), one has $h \to 0$. Hence, from (17), the longitudinal wavenumber converges to its maximum value

$$\beta_{\max} = \sqrt{\frac{\varepsilon_{\|}}{\varepsilon_{\perp}}\left(\varepsilon_{\perp}\mu_{\perp} - \Omega^2\right) - \beta_y^2}. \tag{32}$$

One should note that due to an increased value of the cutoff parameter l/λ_c for the LSM_{11} mode, the range for monomodal operation is increased compared to the nonpseudochiral case, thus allowing a larger bandwidth for single-mode operation.

The variation of the longitudinal wavenumber β with b/λ is shown in Fig. 8, where $b/\lambda = 4.0$ and $\Omega = 1$ were taken. The upper thin line corresponds to the $h = 0$ *loci*, i.e., whenever $b/\lambda \to \infty$. In that case, where β will assume the same value as in (32). On the other hand, the lower thin line is related to the *open-waveguide* cutoff condition $\alpha = 0$, in which

$$\beta = \sqrt{1 - \beta_y^2}. \tag{33}$$

In this case, near cutoff, only the first mode, i.e., the LSM_{01} mode, behaves like a *closed-waveguide* mode.

Finally, Fig. 9 shows the variation of β with Ω for $b/\lambda = 0.4$ and $l/\lambda = 0.5$. One should note that for any LSM mode, there is an upper bound for the magnitude of the pseudochiral parameter Ω, beyond which the mode is at cutoff.

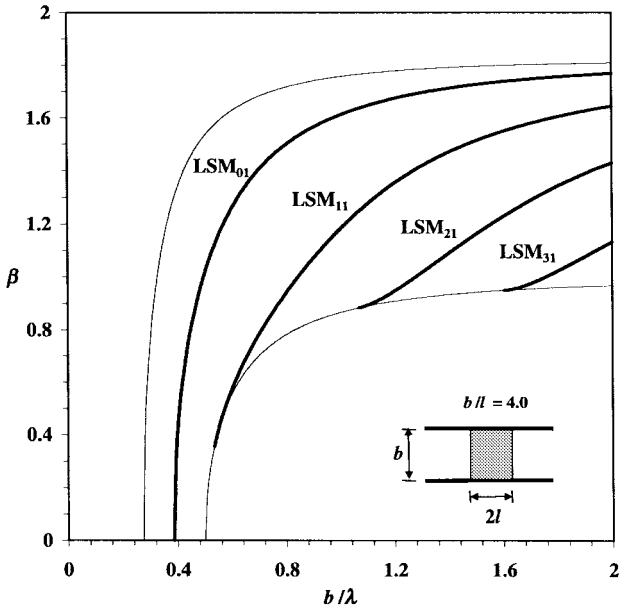

Fig. 8. Variation of the longitudinal wavenumber β with b/λ for LSM modes of an Ω-NRD waveguide, with $\varepsilon_{\|} = 2$, $\varepsilon_{\perp} = 3$, $\mu_{\|} = 1$, and $\mu_{\perp} = 2$ when $b/\lambda = 4.0$ and $\Omega = 1.0$.

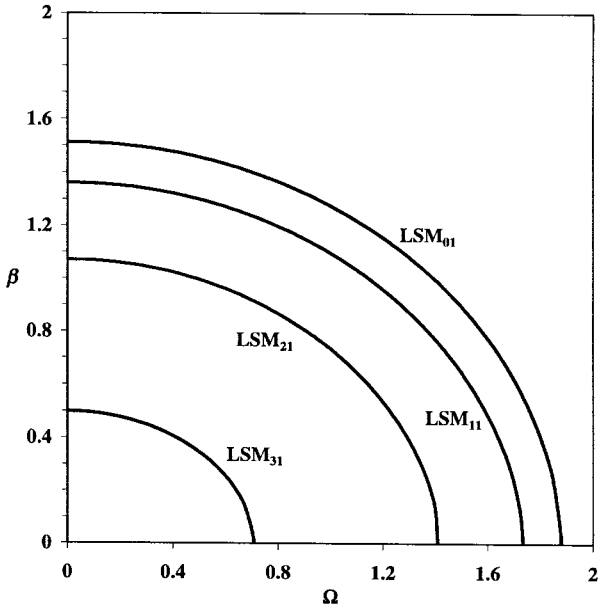

Fig. 9. Variation of the longitudinal wavenumber β with Ω for the first propagating LSM modes of the Ω-NRD waveguide of Fig. 4 when $l/\lambda = 0.5$.

V. Conclusions

In this paper, we have presented a new microwave device: a pseudochiral NRD waveguide, i.e., an NRD waveguide where the usual isotropic slab is replaced by a uniaxial pseudochiral Ω-slab. It was proven that this waveguide supports uncoupled LSE and LSM hybrid modes.

After developing a rigorous full-wave analysis and deriving the modal equations for both LSE and LSM hybrid modes, we focused our attention on the LSM modes. In fact, the LSM_{01} is the most promising mode from the point of view of practical applications.

As this pseudochiral waveguide is a semi-open structure, the cutoff of a given mode can be determined—depending on the b/λ value—either by a closed-waveguide or by an open-waveguide cutoff condition. In the NRD mode of operation (since the distance between the metal plates is less then half a wavelength), the cutoff is determined by the closed-waveguide condition. Dispersion curves as well as operational diagrams were shown for the first LSM propagating modes.

In particular, we have shown that due to the inclusion of Ω-shaped conducting microstructures into the isotropic host medium, new propagation features can be exploited. Namely that, for any LSM mode, there is a bound for the magnitude of the pseudochiral Ω parameter, beyond which the mode is at cutoff. Moreover, there is an upper limit for Ω above which there is no guided-wave propagation. Due to pseudochirality, the bandwidth for single-mode operation can be increased. In fact, whenever $b/\lambda < 0.5$, with the inclusion of the Ω-shaped microstructures there is an increase in the cutoff frequency of the higher order modes (mainly of the second mode, i.e., LSM_{11}), while the fundamental mode LSM_{01} keeps a null cutoff frequency.

Acknowledgment

The authors wish to acknowledge two anonymous reviewers for their contribution to improve the correctness of the analysis.

References

[1] N. Engheta and M. M. Saadoun, "Novel pseudochiral or Ω-medium and its applications," in *Proc. PIERS'91*, Cambridge, MA, July 1991, p. 339.
[2] M. M. I. Saadoun and N. Engheta, "A reciprocal phase shifter using novel pseudochiral or Ω-medium," *Microwave Opt. Technol. Lett.*, vol. 5, pp. 184–188, 1992.
[3] A. Toscano and L. Vegni, "Electromagnetic waves in planar pseudochiral Ω structures," in *Bianisotropic and Bi-isotropic Media and Applications*, A. Priou, Ed. (Progress in Electromagnetic Research Series, PIERS 9). Cambridge, U.K.: EMW Publishing, 1994, pp. 181–218.
[4] M. Norgren and S. He, "Reconstruction of the constitutive parameters for an Ω material in a rectangular waveguide," *IEEE Trans. Microwave Theory Tech.*, vol. 43, pp. 1315–1321, June 1995.
[5] A. Toscano and L. Vegni, "Isotropic-pseudochiral interface characteristics," *J. Electromagnetic Waves Applicat.*, vol. 9, no. 7/8, pp. 1045–1063, 1995.
[6] J. Mazur and D. Pietrzak, "Field displacement phenomenon in a rectangular waveguide containing a thin plate of an Ω medium," *IEEE Microwave Guided Wave Lett.*, vol. 6, pp. 34–36, Jan. 1996.
[7] T. Yoneyama and S. Nishida, "Nonradiative dielectric waveguide for millimeter-wave integrated circuits," *IEEE Trans. Microwave Theory Tech.*, vol. MTT-29, pp. 1188–1192, Nov. 1981.
[8] A. Sanchez and A. A. Oliner, "A new leaky waveguide for millimeter wave using nonradiative dielectric (NRD) waveguide—Part I: Accurate theory," *IEEE Microwave Theory Tech.*, vol. MTT-35, pp. 737–747, Aug. 1987.
[9] H. Qing, A. A. Oliner, and A. Sanchez, "A new leaky waveguide for millimeter wave using nonradiative dielectric (NRD) waveguide—Part II: Comparison with experiments," *IEEE Microwave Theory Tech.*, vol. MTT-35, pp. 748–752, Aug. 1987.
[10] T. Yoneyama, N. Tozawa, and S. Nishida, "Coupling characteristics of nonradiative dielectric waveguides," *IEEE Trans. Microwave Theory Tech.*, vol. MTT-31, pp. 648–654, Aug. 1983.
[11] H. Yoshinaga and T. Yoneyama, "Design and fabrication of a nonradiative dielectric waveguide circulator," *IEEE Trans. Microwave Theory Tech.*, vol. 36, pp. 1526–1529, Nov. 1988.
[12] L. L. Xiao, L. Zhu, and W. X. Zhang, "Analysis of the mono-groove NRD waveguide and antenna," *Int. J. Infrared Millim. Waves*, vol. 10, pp. 361–370, 1989.

[13] F. J. Tisher, "Properties of the H-guide at microwaves and millimeter waves," *Proc. Inst. Elect. Eng.*, vol. 106, pt. B, pp. 47–53, Jan. 1959.
[14] A. César and R. Souza, "Full-wave analysis of a transversely magnetized ferrite nonradiative dielectric waveguide," *IEEE Trans. Microwave Theory Tech.*, vol. 41, pp. 647–651, Apr. 1993.
[15] ———, "Uniaxial anisotropy effect on the nonradiative dielectric (NRD) waveguide performance," in *Proc. PIERS'97*, Hong Kong, Jan. 1997, p. 207.
[16] A. L. Topa, C. R. Paiva, and A. M. Barbosa, "Ω-NRD-guide: Pseudochiral nonradiative dielectric waveguide," in *Proc. APMC'97—Asia–Pacific Microwave Conf.*, Hong Kong, Dec. 1997, p. 597.
[17] S. Tretyakov and A. Sochava, "Proposed composite material for nonreflecting shields and antenna radomes," *Electron. Lett.*, vol. 29, pp. 1048–1049, June 1993.
[18] I. Lindell, S. Tretyakov, and A. Viitanen, "Plane-wave propagation in a uniaxial chiro–omega medium," *Microwave Opt. Technol. Lett.*, vol. 6, pp. 517–520, July 1993.
[19] A. L. Topa, C. R. Paiva, and A. M. Barbosa, "A linear-operator formalism for the analysis of inhomogeneous pseudochiral planar waveguides," in *Dig. North American Radio Sci. Meeting—URSI*, Montreal, P.Q., Canada, July 1997, p. 81.
[20] ———, "Complete spectral representation for the electromagnetic field of planar multi-layered waveguides containing pseudochiral Ω-media," *Progress Electromagnetics Res.*, vol. 18, pp. 85–104, 1998.

António L. Topa was born in Lisbon, Portugal, in 1962. He received the *Licenciado* and Master's degrees in electrical engineering, and the Ph.D. degree from the Instituto Superior Técnico (IST), Technical University of Lisbon, Lisbon, Portugal, in 1985, 1989, and 1998, respectively.

He is currently an Assistant Professor in the Department of Electrical and Computer Engineering, IST, and a Member of the research staff at the Institute for Telecommunications, Lisbon, Portugal. His current research interest is in electromagnetic-wave propagation in planar waveguides containing bianisotropic media and its applications to microwave and integrated optics.

Carlos R. Paiva (S'84–M'90) was born in Lisbon, Portugal, in 1957. He received the *Licenciado*, Master's, and Ph.D. degrees in electrical engineering from the Instituto Superior Técnico (IST), Technical University of Lisbon, Lisbon, Portugal, in 1982, 1986 and 1992, respectively.

He is currently an Associate Professor in the Department of Electrical and Computer Engineering, IST, and a Member of the research staff at the Institute for Telecommunications, Lisbon, Portugal. His current research interests include electromagnetic-wave theory of complex media and its applications to microwave engineering and integrated optics, and nonlinear fiber optics and its applications to soliton communication systems and photonic switching.

Afonso M. Barbosa (S'80–A'83–SM'90) was born in Coimbra, Portugal, in 1950. He received the *Licenciado* degree in electrical engineering from the Instituto Superior Técnico (IST), Technical University of Lisbon, Lisbon, Portugal, in 1972, the Master's degree in electronic engineering from NUFFIC, Eindhoven, The Netherlands, in 1972, and the Ph.D. degree from IST, in 1984.

He is currently a Full Professor in the Department of Electrical and Computer Engineering, IST, and a Member of the research staff and Executive Board at the Institute for Telecommunications, Lisbon, Portugal. His current research interests are in electromagnetic-wave theory and applications, namely microwave, millimeter-wave and optical waveguide structures, and antennas and scattering with emphasis on complex media.